Bisimide–Lactamimide ring contraction in six-membered bisimides: a theoretical study

Patricia Ponce, Lioudmila Fomina and Serguei Fomine*

Instituto de Investigaciones en Materiales, Universidad Nacional Autónoma de México, Apartado Postal 70–360, CU, Coyoacán, México DF 04510, México

ABSTRACT: The bisimide–lactamimide ring contraction reaction of six-membered bisimides has been modeled at the B3PW91/6-31 + G(d,p)//HF/3-21G level of theory using the isodensity polarized continuum model to take into account the solvent effect. Basically, the results of molecular modeling support the validity of the proposed mechanism. However, the calculations suggest that the final reaction step involves the direct oxidation of dianions by molecular oxygen, instead of oxidation of the hydroaromatic intermediate as proposed previously. The reactivity difference between *N*-alkyl and *N*-phenyl bisimides in the ring contraction reaction has been explained. Copyright © 2001 John Wiley & Sons, Ltd.

KEYWORDS: ring contraction; bisimides; lactamimides; molecular modeling; DFT calculations

INTRODUCTION

Six-membered ring dicarboximides are commonly viewed as chemically very inert. Strong hydrolyzing reagents such as hot, concentrated sulfuric acid or KOH in t-BuDH alcohol are required for their saponification.[1] A completely different reaction pathway is observed, however, if alkali metal hydroxides in methanol react with six-membered bisimides, such as naphthalene-1,8:4,5-bisimides (Scheme 1). In this case, lactamimides are produced[2] with the loss of a C1 fragment from one carboximide. Whereas the reaction of bisimides with KOH in t-BuOH leads to their hydrolysis, in methanol the ring contraction is the predominant reaction pathway. Addition of dimethylsulfoxide (DMSO) further increases the yield and shortens the reaction times.
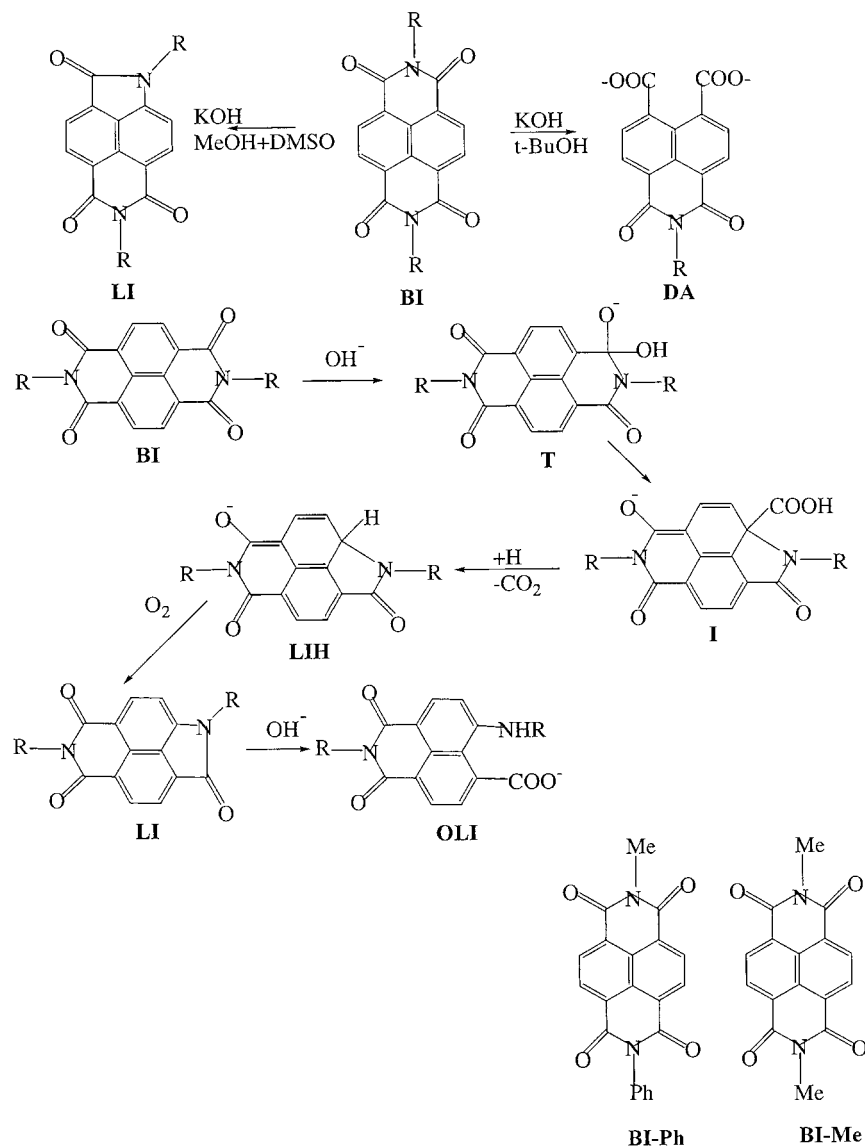
The ring contraction reaction proceeds quite easily for R=aryl, but it is more difficult for R=alkyl. Only one of the imide rings is transformed, leaving the second one unchanged even under more vigorous conditions; however, a second imide unit is essential for the reaction to occur. In agreement with this, monoimides do not undergo ring contraction. On the basis of these findings, the following mechanism has been proposed (Scheme 1).[2] The reaction is initiated by the addition of OH⁻ to one of the imide carbonyl groups to form tetrahedral

intermediate **T**. This intermediate is converted to **I**, followed by the formation of **LIH**. Decarboxylated product **LIH** is a hydroaromatic species that is oxidized by air to generate lactamimide **LI**. This ring contraction reaction can be successfully extended to other bisimides[3–5] and, therefore, appears to be a general reaction. Lactamimides show remarkable photostability and strong fluorescence, rendering them as a novel class of fluorescent dyes,[2] and the detailed study of the reaction mechanism is essential for the tailoring of novel lactamimides. The aim of this paper is to study the mechanism of the ring contraction reaction using quantum chemistry tools.

COMPUTATIONAL DETAILS

The A9 revision of Gaussian 98[6] was used to carry out all calculations. All geometry optimizations were run at the HF/3-21G level. To test the validity of this model for the geometry optimization, first, molecule **I** was minimized at the B3LYP/6-31 + G(d) level[7,8] and the results were compared to these obtained at HF/3-21G level. All bond lengths and angles were reproduced within 0.02 Å and 2° respectively. Each stationary point was characterized by frequency calculations to ensure that a minimum (no imaginary modes) or a transition state (one imaginary mode) had been located. Zero-point energies were scaled by a factor of 0.9409[9] and used to correct the total energies. Single-point energy calcula-

Copyright © 2001 John Wiley & Sons, Ltd.

J. Phys. Org. Chem. 2001; **14:** 657–666

Scheme 1. The ring contraction mechanism proposed by Linghals and Unhold[2]

tions were run using Becke's three-parameter hybrid functional[7] with the Perdew/Wang91 correlation functional[10] using the 6-31 + G (d,p) basis set at HF/3-21G optimized geometries. Solvation energies were calculated at the B3PW91/6-31 + G(d,p) level of theory using the isodensity polarized continuum model (IPCM).[11] To model the mixture of MeOH and DMSO commonly used for the ring contraction reaction, a dielectric constant of 40 was used.

A time-dependent (TD) B3LYP functional in combination with 6-31 + G(d,p) basis set has been used to simulate the visible absorption spectra of the reactive intermediates. It has been shown that this method reproduces very well the absorption maxima of substituted lactamimides.[12]

RESULTS AND DISCUSSION

In order to elucidate the difference between aliphatic and aromatic substituents in the ring contraction reaction, two different bisimide molecules were used as models (Scheme 1); **BI—Me** and **BI—Ph**. The hydrolysis, as well as the ring contraction reaction, starts with the formation of tetrahedral intermediate **I** (Fig. 1) or **I—Ph** (Fig. 2). The attack of the imide nitrogen at the naphthalene carbon to form intermediates **III** or **III—Ph** leads to the ring contraction, whereas cleavage of the **N—C** bond in molecules **I** and **I—Ph** results in hydrolysis. Total and solvation energies of calculated molecules are listed in Tables 1 and 2, and the reaction energies are presented in Table 3. Scheme 2 presents
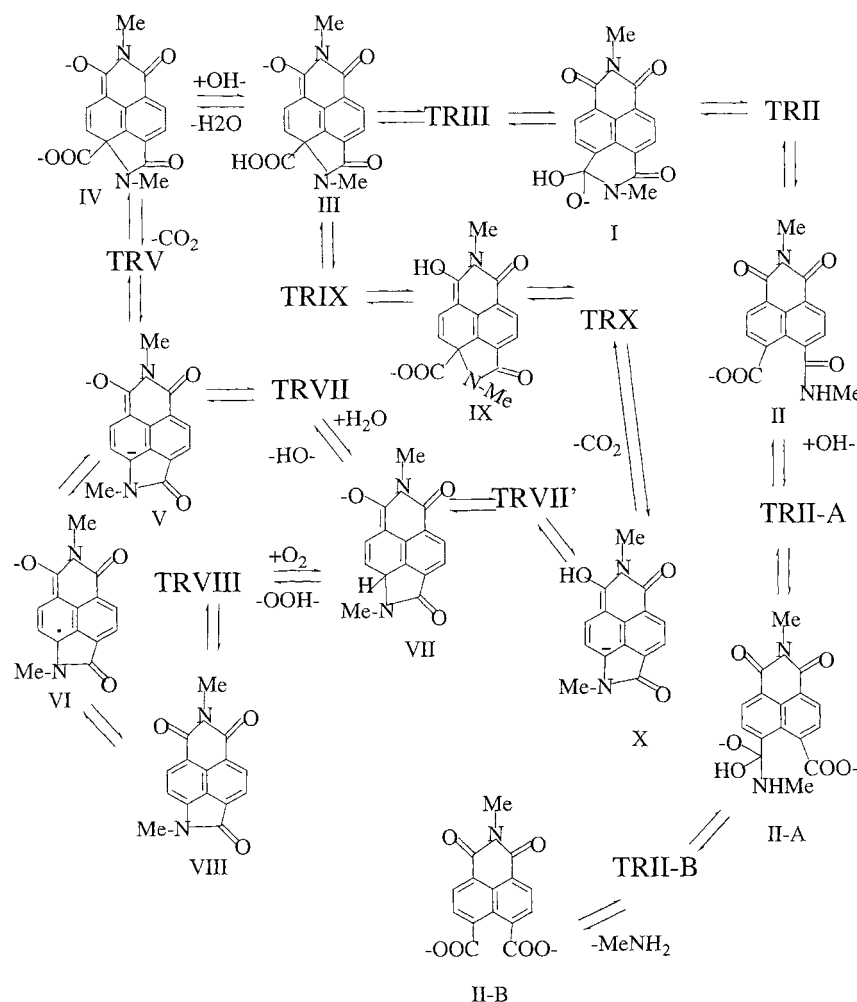
Figure 1. Reaction pathways for N,N-dimethylnaphthalene-1,4,5,8-tetracarboxylic acid bisimide

the relative energies of the most important reaction species.

The first step of hydrolysis (**I–II** transformation) is favored thermodynamically and kinetically in the gas phase over that of **I–III** (Table 3), but the next step, starting with the formation of tetrahedral intermediate **II—A**, is an endothermic process with high activation energy. The last step of hydrolysis (**II—A–II—B** transformation) is exothermic with an activation energy of 24.1 kcal mol^{-1}. Therefore, the rate-determining step for hydrolysis is the formation of tetrahedral intermediates **II—A** and **II—A—Ph**, in agreement with experimental data for amide hydrolysis.[13] The gas-phase calculations reveal that bisimide with R=Ph is easier to hydrolyze compared with R=Me. The **I—Ph–II—Ph–II—A—Ph–II—B** reaction sequence has lower activation energies in comparison with similar sets of reactions for aliphatic lactamimide. A better nucleofugacity for PhNH$_2$ compared with MeNH$_2$ is responsible for this. Solvation affects aliphatic and aliphatic–aromatic bisimides in different ways. In the case of aliphatic bisimide

solvation favors the hydrolysis thermodynamically and kinetically, whereas for molecule **I—Ph** the first step of the hydrolysis, namely the formation of the **II—Ph** intermediate, becomes less exothermic and the activation energy of this process increases, reflecting the weaker solvation of the **II—Ph** and **TRII—Ph** intermediates compared with their aliphatic analogues. The formation of intermediate **III** is an endothermic process in the gas phase, whereas the similar reaction producing intermediate **III—Ph** is exothermic. Moreover, the **I—Ph–III—Ph** transformation activation energy is smaller than that for the reaction **I–III** by a factor of two. Solvation only slightly destabilizes **III—Ph**, whereas for **III** the destabilization is more pronounced (Table 3). Therefore, the ring contraction reaction is more favorable for bisimides bearing phenyl substituents, in agreement with experimental observations.

According to the proposed mechanism,[2] intermediates **III** and **III—Ph** are to transform into hydroaromatic intermediates **VII** and **VII—Ph**. However, given the reaction medium is very basic, the carboxylic proton will
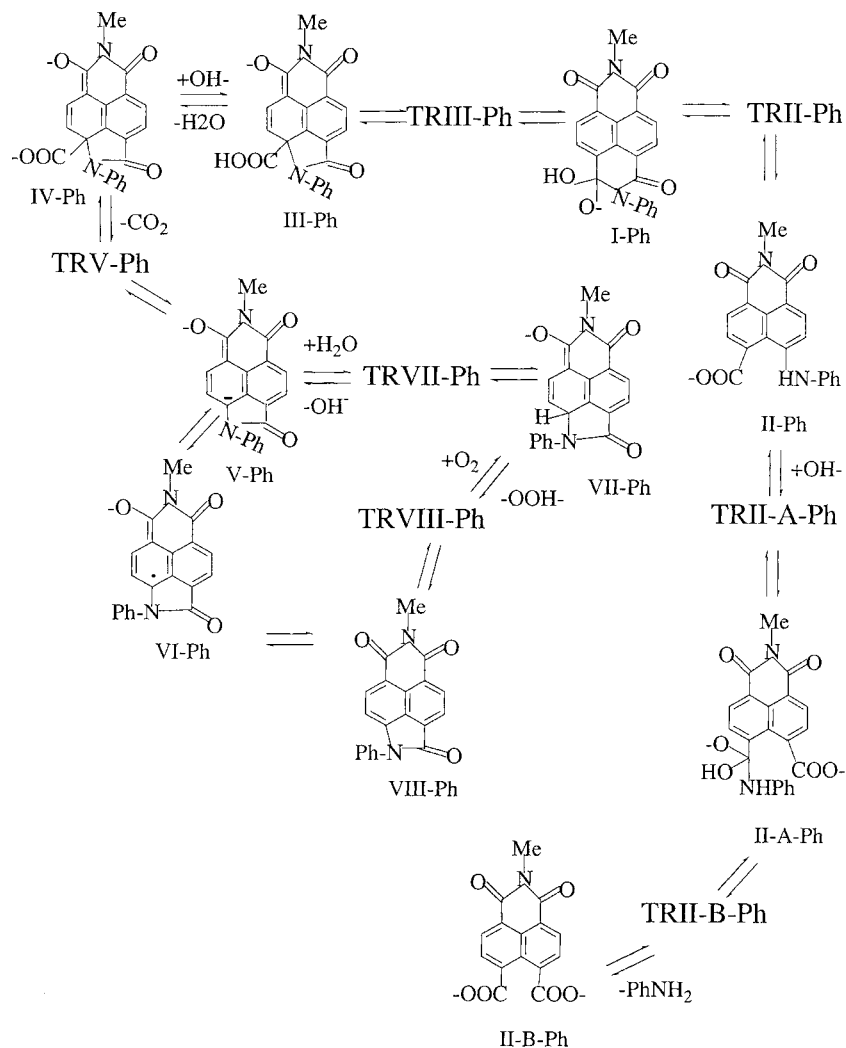
Figure 2. Reaction pathways for *N*-methyl-*N*'-phenylnaphthalene-1,4,5,8-tetracarboxylic acid bisimide

immediately be abstracted to produce intermediates **IV** and **IV—Ph** respectively. These reactions proceed very easily, since no transition states were detected either for the transformations **4** or for **17** (Table 3). A relaxed potential energy scan performed for the reaction **III** + OH⁻ = **IV** + H₂O at the B3PW91/6-31G(d)//HF/3-21G level of theory (Fig. 3) showed that the gas-phase reaction proceeded with no activation energy. When solvation in a DMSO–MeOH mixture is taken into account, a small barrier of just 3.4 kcal mol⁻¹ appears at COO—H distance of 1.393 Å.

An alternative proton abstraction scheme is shown in Fig. 1, where protons are transferred from the carboxyl oxygen to the closest imide carbonyl oxygen (reaction **III–IX**). According to the theoretical model applied, this reaction has an activation energy of 35.8 kcal mol⁻¹ in the gas phase and the solvation barely affects this value (Table 3). Moreover, this reaction is only slightly exothermic in a DMSO–MeOH mixture. Therefore, the **III–IV** and **III—Ph–IV—Ph** pathways are favored in this case.

IV and **IV—Ph** intermediates generate dianions **V** and **V—Ph** with loss of CO₂. The decarboxylation is much more favorable thermodynamically and kinetically for aromatic intermediate **IV—Ph**. This difference can be explained by two factors. The first one is that the more hydrophilic molecule **IV** and transition state **TRV** are better solvated compared with those of **IV—Ph** and **TRV—Ph**. The second one is that phenyl ring stabilizes the excessive negative charge of the dianion, judging from the significant decrease in the dihedral angle between the lactamimide and phenyl ring planes in **V—Ph** (28.6°) compared with the uncharged lactamimide **VIII—Ph** (52.3°) (Fig. 4). This hypothesis is also confirmed by the partial charges analysis in the **V—Ph** and **VIII—Ph** molecules. Mulliken-, ESP- and NBO-derived charges on the phenyl group in **V—Ph** are more negative (by 0.17–0.28*e*) compared with those of **VIII—**

Table 1. Zero point, total and solvation energies of N,N'-dimethyl substituted intermediates (hartree)

Molecule	ZPE[a]	E + ZPE[b]	S-1[c]	S-2[d]
I	0.253 032	−1101.469 998	−0.084 302	−0.072 190
II	0.253 330	−1101.479 597	−0.089 242	−0.076 334
TRII-A	0.262 638	1177.162 715	−0.269 637	−0.233 303
II-A	0.265 324	−1177.180 677	−0.275 693	−0.238 084
TRII-B	0.260 970	−1177.142 281	−0.268 362	−0.233 463
II-B	0.197 970	−1081.441 412	−0.309 796	−0.265 972
III	0.252 635	−1101.468 554	−0.079 202	−0.067 8874
IV	0.239 332	−1100.842 595	−0.269 478	−0.233 622
V	0.224 256	−912.331 447	−0.262 626	−0.229 160
VII	0.237 790	−912.973 552	−0.079 521	−0.069 003
VIII	0.229 517	−912.324 781	−0.019 761	−0.016 733
IX	0.251 913	−1101.435 752	−0.118 245	−0.097 369
X	0.236 496	−912.949 335	−0.093 863	−0.079 839
TRIII	0.250 115	−1101.436 585	−0.083 983	−0.072 031
TRII	0.251 021	−1101.448 783	−0.081 433	−0.068 844
TRIX	0.247 248	−1101.411 533	−0.078 246	−0.067 887
TRV	0.235 916	−1100.831 978	−0.255 136	−0.221 670
TRX	0.248 711	−1101.439 319	−0.094 182	−0.079 361
TRVII′	0.230 023	−912.803 739	−0.082 708	−0.071 075
TRVII	0.244 744	−988.688 474	−0.254 179	−0.222 307
TRVIII	0.239 715	−1063.203 478	−0.084 302	−0.072 031
VI	0.225 179	−912.405 736	−0.079 361	−0.068 844

[a] Scaled zero point energy (ZPE) at the HF/3-21G level of theory. Scaling factor is 0.9409.[9]
[b] ZPE-corrected B3PW91/6-31 + G(d,p)//HF/3-21G total energies.
[c] Solvation energies calculated at B3PW91/6-31(d,p)//HF/3-21G level of theory using Tomasi's IPCM with a dielectric constant of 40.0 for the MeOH–DMSO mixture.
[d] Solvation energies calculated at the B3PW91/6-31(d,p)//HF/3-21G level of theory using Tomasi's IPCM with a dielectric constant of 7.0 for t-BuOH.

Table 2. Zero point, total and solvation energies of N-methyl,N-phenyl substituted intermediates (hartree)

Molecule	ZPE[a]	E + ZPE[b]	S-1[c]	S-2[d]
I—Ph	0.306 698	−1293.078 606	−0.091 951	−0.076 812
II—Ph	0.308 260	−1293.101 321	−0.083 823	−0.071 393
TRII—A—Ph	0.317 357	−1368.799 659	−0.258 004	−0.223 264
II—A—Ph	0.319 894	−1368.8258	−0.242 387	−0.210 196
TRII—B—Ph	0.315 548	1368.822 312	−0.238 881	−0.207 487
III—Ph	0.306 430	−1293.079 528	−0.087 807	−0.074 262
IV—Ph	0.293 736	−1292.466 048	−0.253 861	−0.219 598
V—Ph	0.278 656	−1103.959 185	−0.260 235	−0.225 176
VII—Ph	0.291 993	−1104.588 332	−0.090 357	−0.076 652
VIII—Ph	0.283 361	−1103.938 778	−0.028 047 4	−0.021 992
TRIII—Ph	0.304 659	−1293.060 902	−0.083 345 3	−0.070 915
TRII—Ph	0.305 674	−1293.075 403	−0.084 620 2	−0.066 772
TRV—Ph	0.290 416	−1292.459 547	−0.251 152	−0.216 889
TRVII—Ph	0.298 369	−1180.316 469	−0.256 251	−0.225 654
TRVIII—Ph	0.293 785	−1254.820 676	−0.093 863	−0.078 246
VI—Ph	0.279 393	−1104.023 184	−0.084 779 6	−0.072 350

[a] Scaled zero point energy (ZPE) at the HF/3-21G level of theory. Scaling factor is 0.9409.[9]
[b] ZPE-corrected B3PW91/6-31 + G(d,p)//HF/3-21G total energies.
[c] Solvation energies calculated at the B3PW91/6-31(d,p)//HF/3-21G level of theory using Tomasi's IPCM with a dielectric constant of 40.0 for the MeOH–DMSO mixture.
[d] Solvation energies calculated at the B3PW91/6-31(d,p)//HF/3-21G level of theory using Tomasi's IPCM with a dielectric constant of 7.0 for t-BuOH.

Ph. Moreover, the N—C_{ar} bond is shorter by 0.05 Å in V—Ph, suggesting some contribution from the quinone structure, which is in agreement with delocalization of the π-electron density by the phenyl ring in the dianions.

There are two possible reaction pathways to convert **V** and **V—Ph** dianions into lactamimides **VIII** and **VIII— Ph** (Figs 1 and 2). The first one is proton abstraction from a solvent molecule to generate intermediates **VII** and

Table 3. Reaction (ΔE) and activation (E_a) energies calculated at the B3PW91/6-31 + G(d,p)//HF/3-21G level of theory in the gas phase and solution
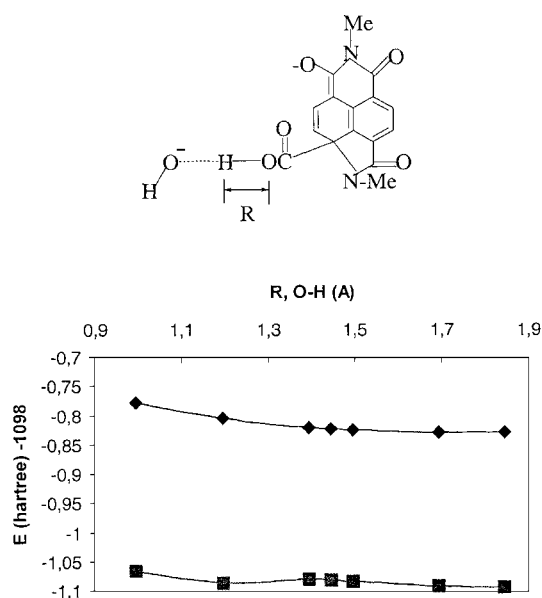
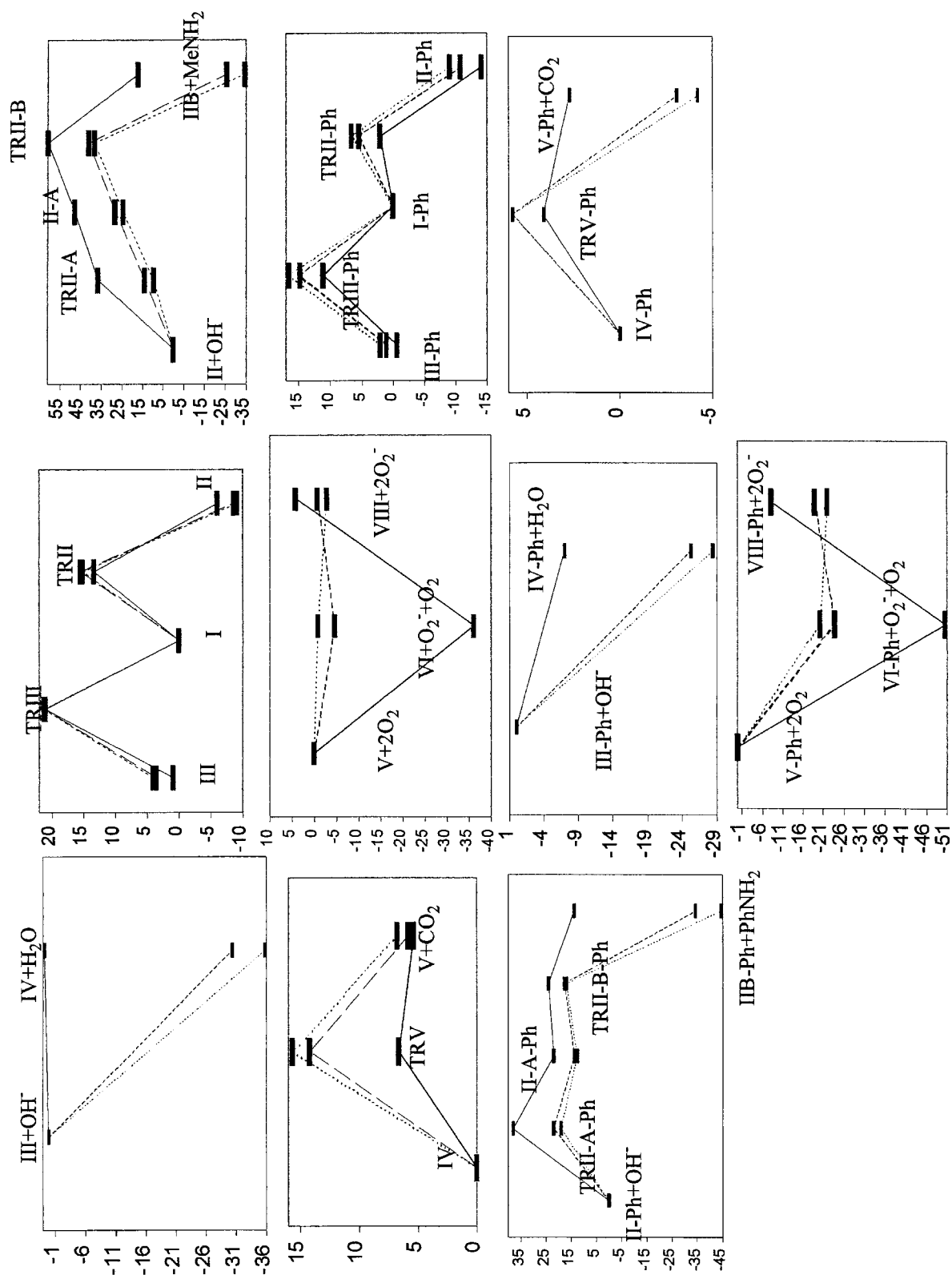| Reaction	ΔE (kcal mol^{-1})			E_a (kcal mol^{-1})		
	Gas phase	MeOH–DMSO	t-BuOH	Gas phase	MeOH–DMSO	t-BuOH
I=II	−6.0	−9.1	−8.6	13.3	15.1	15.4
1. II + OH$^-$=II—A	36.5	9.6	13.9	47.8	24.7	28.2
2. II—A=II—B + MeNH$_2$	−19.4	−44.4	−39.9	24.1	28.7	27.0
3. I=III	0.9	4.1	3.6	21.0	21.2	21.1
4. III + OH$^-$=IV + H$_2$O	0.8	−35.8	−30.4	–	–	–
5. IV=V + CO$_2$	5.4	6.8	5.9	6.7	15.7	14.2
6. V + H$_2$O=VII + OH$^-$	−10.9	21.2	16.7	16.9	28.2	27.2
7. VII + O$_2$=VIII + OOH$^-$	24.7	−22.2	−16.1	21.1	18.1	19.2
8. III=IX	20.5	−4.0	2.0	35.8	36.4	35.8
9. IX=X + CO$_2$	−10.1	2.3	−2.0	−2.2	12.9	9.1
10. X=VII	−15.2	−6.1	−8.4	91.4	98.4	96.9
11. V + O$_2$ = VI + O$_2{}^-$	−36.1	−0.8	−4.6	–	–	–
12. VI + O$_2$ = VIII + O$_2{}^-$	40.3	−2.0	3.9	–	–	–
13. I—Ph=II—Ph	−14.2	−9.1	−10.8	2.0	6.6	5.4
14. II—Ph + OH$^-$=II—A—Ph	21.8	12.4	13.6	38.2	19.0	21.8
15. II—A—Ph=II—B + PhNH$_2$	−8.1	−56.9	−48.1	2.2	4.4	3.9
16. I—Ph=III—Ph	−0.6	2.0	1.0	11.1	16.5	14.8
17. III—Ph + OH$^-$=IV—Ph + H$_2$O	−7.0	−28.4	−25.3	–	–	–
18. IV—Ph=V—Ph + CO$_2$	2.7	−4.2	−3.1	4.1	5.8	5.8
19. V—Ph + H$_2$O=VII—Ph + OH$^-$	−2.8	21	20.3	16.7	26.5	22.4
20. VII—Ph + O2=VIII—Ph + OOH$^-$	31.4	−13.9	−7.9	19.5	17.3	18.5
21. V–Ph + O$_2$ = VI–Ph + O$_2{}^-$	−50.6	−20.2	−23.8	–	–	–
22. VI–Ph + O$_2$ = VIII–Ph + O$_2{}^-$	42.5	−1.6	5.0	–	–	–

VII—Ph followed by their oxidation by atmospheric oxygen (reactions **6, 7** and **19, 20**, Table 3). The second one is direct oxidation of dianions **V** and **V—Ph** by molecular oxygen (reactions **11, 12** and **21, 22**, Table 3). As seen from the Table 3, dianions are stronger bases than OH$^-$ in the gas phase (a similar situation holds for MeO$^-$). However, neither **V** nor **V—Ph** are able to abstract protons from water in solution owing to the strong stabilization of these dianions by solvent molecules. An alternative way to form hydroaromatic intermediate involves the reaction path **III–IX–X–VII**. However, the reactions **III–IX** and especially **X–VII** show much higher activation energies compared with the **III–IV–V** route; therefore, it is difficult to expect them to occur. It seems that the most probable reaction pathway is the direct oxidation of dianions **V** and **V—Ph** by molecular oxygen.

With the proviso that the oxidation reaction involves two one-electron transfers from a dianion to two oxygen molecules, one can see that the formation of anion-radicals **VI** and **VI—Ph** is thermodynamically favored in the gas phase and in solution, whereas the oxidation of anion-radicals to lactamimides **VIII** and **VIII—Ph** is only possible in a DMSO–MeOH mixture, not in t-BuOH, because of the difference in solvation energies. This finding agrees very well with the fact that MeOH or the DMSO–MeOH mixed solvent favors the ring contraction, whereas t-BuOH does not.

To support this hypothesis an attempt has been made to

detect dianion **V** by UV–visible spectroscopy during the ring contraction reaction. Table 4 presents the calculated wavelengths and oscillator strengths of the lowest allowed transitions for molecules **V, VI, VII** and **OLI**

Figure 3. Relaxed potential energy surface scan for carboxylic proton abstraction from intermediate **III** by OH$^-$ at the B3PW91/6-31G(d)//HF/3-21G level: ◆, gas phase; ■, DMSO–MeOH mixture (IPCM)

Scheme 2. Energy diagram showing relative energies (kcal mol^{-1}) of the most important reaction species: (——) gas phase, (.....) t-BuOH, (———) MeOH–DMSO mixture
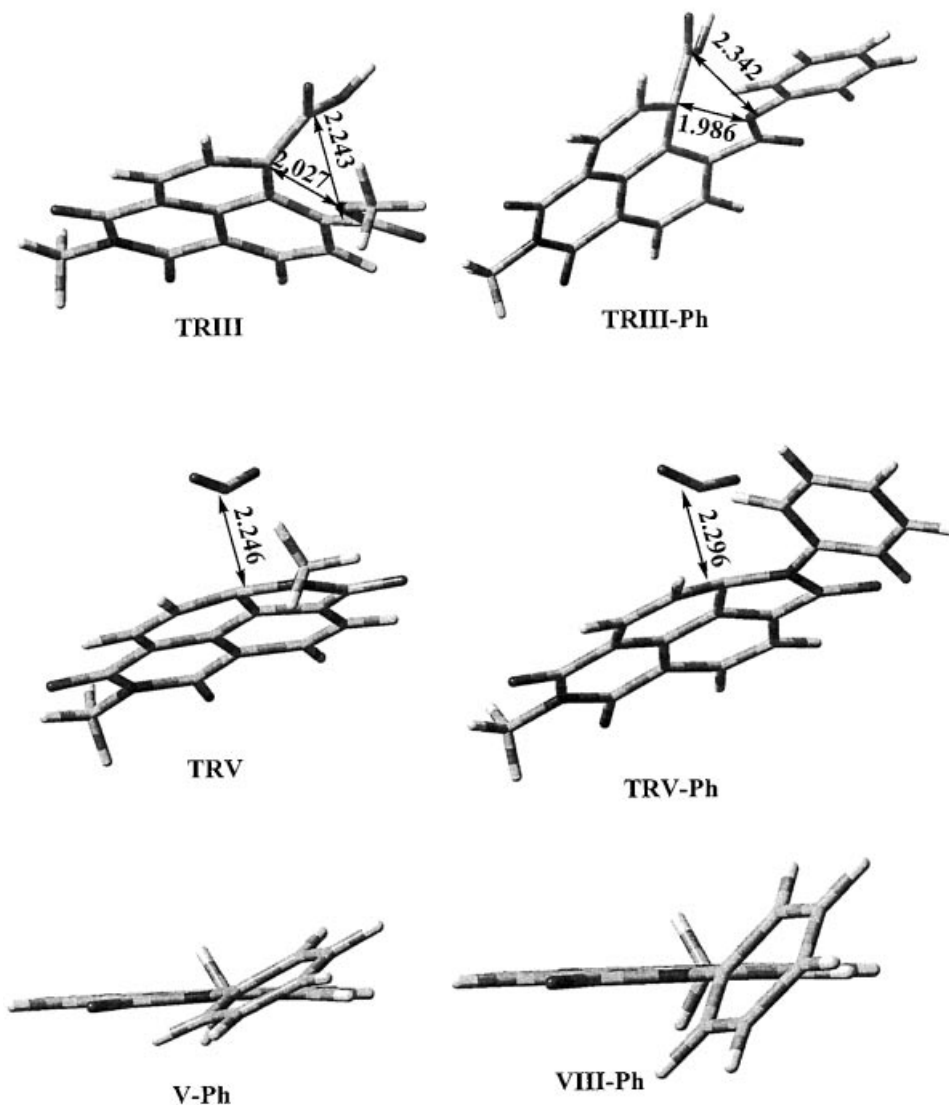
Figure 4. Stationary-point geometries for some of the intermediates of the bisimide–lactamimide ring contraction reaction with the respective interatomic distances (Å)

at the TD-B3LYP/6–31 + G(d,p)//HF/3–21G level of theory, as well as the absorption maxima of the reaction mixture during the ring contraction of N',N-bis(6-hydroxyhexyl)-1,8,4,5-naphthalenetetracarboxylic bisimide (Scheme 1, **BI** (R=(CH$_2$)$_6$OH). Fortunately, there is an appreciable difference between the calculated spectra of dianion **V** and hydroaromatic species **VII**. Whereas dianion **V** shows a long wavelength absorption maximum well beyond 500 nm, the only allowed transition in the visible region for molecule **VII** is located at 501 nm. As can be seen from Table 4, there is good agreement between the simulated and experimental spectra of dianion **V**, whereas no absorption band has been detected corresponding to hydroaromatic species **VII**. Two close intense peaks at 475 nm and 451 nm can be assigned to intermediates **V** and **OLI** (Scheme 1) respectively, on the basis of their oscillator strengths.

The accuracy of the model adopted can be tested by comparing the experimentally measured and simulated spectra of the **OLI** molecule formed after the cleavage of lactamimide **LI** by OH$^-$, present in the reaction mixture. This compound is formed when N,N'-bis(6-hydroxyhexyl)-1-amino-4,5,8-naphthalenetricarboxylic acid-1,8-lactam-4,5-imide, obtained as described in the literature,[3] is dissolved in 5% KOH MeOH–DMSO solution. The visible spectrum of this solution shows only one strong absorption band, peaking at 451 nm. Similar absorption spectra for cleaved lactamimide have also been reported.[2] As can be seen from Table 4, the B3PW91/6–31 + G(d,p)//HF/3–21G model reproduces these data fairly well.

Given the fact that hydroaromatic intermediate **VII** has not been detected during the ring contraction[2] and that both molecular modeling and UV–visible spectroscopy

Table 4. Calculated wavelengths λ and oscillator strengths f of lowest allowed transitions for molecules **V, VI, VII** at the TD-B3LYP/6-31 + G(d,p)//HF/3-21G level of theory and experimentally observed visible spectrum of reaction mixture[a]

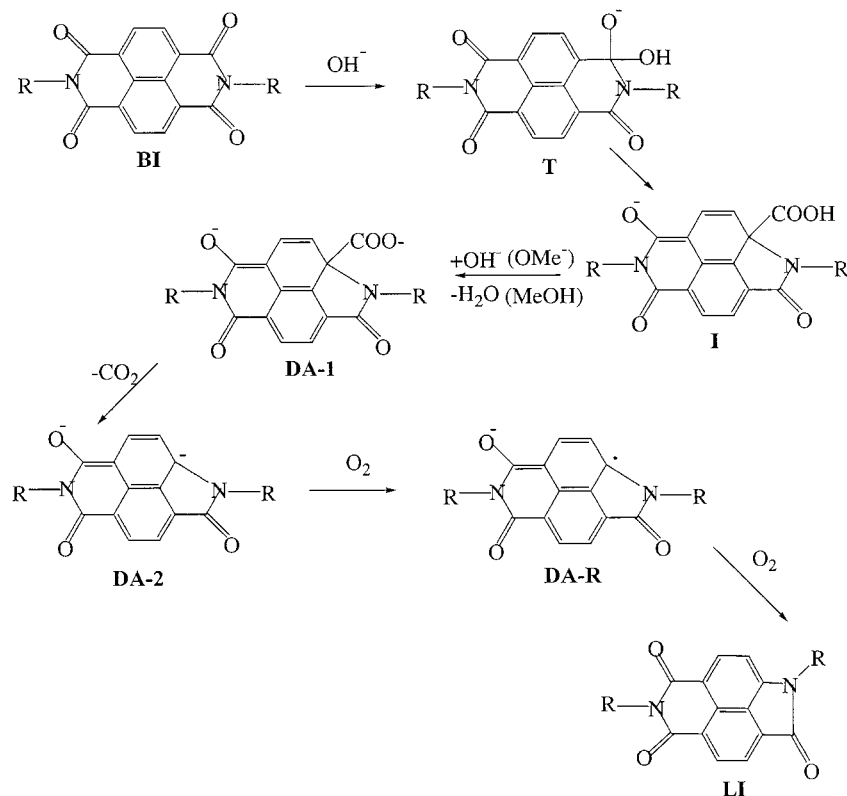| Molecule	f	λ (nm) Calculated	Measured
V	1×10^{-4}	791	760 (weak)
	5×10^{-3}	683	683 (weak)
	2.5×10^{-3}	633	610 (weak)
	1.7×10^{-2}	538	550 (moderate)
	8×10^{-4}	506	
	1.6×10^{-3}	486	
	2.1×10^{-3}	483	
	1×10^{-4}	467	
	0.13	461	475 (strong)
VI	9.7×10^{-2}	569	
	1.4×10^{-2}	538	
	5.2×10^{-2}	504	
	1×10^{-4}	500	
	0.15	422	430 (moderate)
	1×10^{-4}	408	
VII	5.0×10^{-2}	501	
OLI (R=Me)	0.21	438	450 (strong)

[a] UV–visible spectra were taken in DMSO during the ring contraction reaction of N',N-bis(6-hydroxyhexyl)-1,8,4,5-naphthalenetetracarboxylic bisimide (0.528 g) carried out in the presence of KOH (2.0 g), DMSO (8 ml) and MeOH (25 ml)

data favor the reaction pathway involving direct oxidation of dianion **V** by atmospheric oxygen, the ring contraction reaction mechanism can be modified as follows (Scheme 3). The first two steps are similar to those proposed previously,[2] followed by the intermolecular, not intramolecular, deprotonation of the carboxylic group by OH^- or OMe^-. Upon the decarboxylation of intermediate **DA-1**, dianion **DA-2** is directly oxidized by atmospheric oxygen to lactamimide, *via* anion-radical **DA-R**.

CONCLUSIONS

Basically, the results of molecular modeling support the proposed mechanism of the bisimide–lactamimide ring contraction. However, it seems that no hydroaromatic intermediate **VII** is involved in the ring contraction reaction, since both the theoretical and experimental results suggest direct oxidation of dianion **V** and **V—Ph** to lactamimide **VIII** and **VIII—Ph**. The molecular modeling data predict that aromatic substituents at imide nitrogen favor the ring contraction reaction, stabilizing the excessive negative charge.

The last step of the ring contraction reaction, oxidation of dianions **V** and **V—Ph** by atmospheric oxygen, is only

Scheme 3. Possible ring contraction mechanism in agreement with molecular modeling data

possible in DMSO–MeOH mixture, not in t-BuOH, due to the difference in solvation energies. This finding explains why almost no ring contraction occurs in t-BuOH and why the yields of lactamimides increase in going from t-BuOH, EtOH, MeOH to an MeOH–DMSO mixture, in line with the solvent dielectric constants.

Acknowledgements

REFERENCES

1. Linghals H. *Heterocycles* 1995; **40**: 477.
2. Linghals H, Unhold P. *Angew. Chem. Int. Ed. Engl.* 1995; **34**: 2234.
3. Fomine S, Fomina L, Garcia V, Gaviño R. *Polymer* 1998; **39**: 6415.
4. Fomine S, Fomina L, Arreola R, Alonso J. *Polymer* 1999; **40**: 2051.
5. Fomina L, Fomine S, Peña P, Ogawa T, Alexandrova L, Gaviño R. *Macromol. Chem. Phys.* 1999; **200**: 239.
6. Frisch MJ, Trucks GW, Schlegel HB, Scuseria GE, Robb MA, Cheeseman JR, Zakrzewski VG, Montgomery Jr JA, Stratmann RE, Burant JC, Dapprich S, Millam JM, Daniels AD, Kudin KN, Strain MC, Farkas O, Tomasi J, Barone V, Cossi M, Cammi R, Mennucci B, Pomelli C, Adamo C, Clifford S, Ochterski J, Petersson GA, Ayala PY, Cui Q, Morokuma K, Malick DK, Rabuck AD, Raghavachari K, Foresman JB, Cioslowski J, Ortiz JV, Baboul AG, Stefanov BB, Liu G, Liashenko A, Piskorz P, Komaromi I, Gomperts R, Martin RL, Fox DJ, Keith T, Al-Laham MA, Peng CY, Nanayakkara A, Challacombe M, Gill PMW, Johnson B, Chen W, Wong MW, Andres JL, Gonzalez C, Head-Gordon M, Replogle ES, Pople JA. Gaussian 98, Revision A.9. Gaussian, Inc., Pittsburgh, PA, 1998.
7. Becke A. *Phys. Rev. A* 1988; **38**: 3098.
8. Lee C, Yang W, Parr R. *Phys. Rev. B* 1988; **37**: 785.
9. Pople JA, Scott AP, Wong MW, Random L. *Isr. J. Chem.* 1993; **33**: 345.
10. Perdew JP, Burke K, Wang Y. *Phys. Rev. B* 1996; **54**: 16533.
11. Foresman JB, Keith TA, Wiberg KB, Snoonian J, Frisch MJ. *J. Phys. Chem.* 1996; **100**: 16098.
12. Fomina L, Porta B, Acosta A, Fomine S. *J. Phys. Org. Chem.* 2000; **13**: 1.
13. March J. *Advanced Organic Chemistry*. Wiley: New York, 1985; 237–250.